How to cite:
doi.org/10.1002/anie.202300892

Li-Ion Batteries

# Cyclotetrabenzil Derivatives for Electrochemical Lithium-Ion Storage

*Jianing Meng[+], Alexandra Robles[+], Said Jalife[+], Wen Ren[+], Ye Zhang, Lihong Zhao, Yanliang Liang,* Judy I. Wu,* Ognjen Š. Miljanić,* and Yan Yao**

*Dedicated to Professor Fraser Stoddart on the occasion of his 81st birthday*

**Abstract:** Organic electrode materials could revolutionize batteries because of their high energy densities, the use of Earth-abundant elements, and structural diversity which allows fine-tuning of electrochemical properties. However, small organic molecules and intermediates formed during their redox cycling in lithium-ion batteries (LIBs) have high solubility in organic electrolytes, leading to rapid decay of cycling performance. We report the use of three cyclotetrabenzil octaketone macrocycles as cathode materials for LIBs. The rigid and insoluble naphthalene-based cyclotetrabenzil reversibly accepts eight electrons in a two-step process with a specific capacity of 279 mAh $g^{-1}$ and a stable cycling performance with ≈65 % capacity retention after 135 cycles. DFT calculations indicate that its reduction increases both ring strain and ring rigidity, as demonstrated by computed high distortion energies, repulsive regions in NCI plots, and close [C···C] contacts between the naphthalenes. This work highlights the importance of shape-persistency and ring strain in the design of redox-active macrocycles that maintain very low solubility in various redox states.

Electrochemical energy storage systems such as rechargeable batteries have been regarded as one of the most efficient methods to regulate the output of electricity.[1,2] Among these systems, state-of-the-art lithium-ion batteries (LIBs) are widely used as power sources for a plethora of mobile electronic devices and electric vehicles.[3] Traditional LIBs based on transition metal oxide cathodes and graphite anodes are approaching their performance limits,[4,5] and present concerns about the environmental and social impacts of mining materials such as cobalt.[6] It is therefore crucial to develop new, environmentally friendly battery materials with tunable properties.[7,8] Organic rechargeable batteries utilize redox-active organic molecules to store and release charges on demand, offering the promise of sustainable energy storage.[9–11]

Over the past two decades, organic small molecules with various redox characteristics have been investigated as electrode materials for LIBs.[12–14] While these materials are easy to synthesize and have tunable electronic properties, they are often highly soluble in common battery electrolyte solvents, such as organic carbonates and ethers. This solubility leads to rapid capacity decay during cycling tests.[15] To address this issue, researchers have turned to shape-persistent, symmetric, macrocyclic compounds. They combine the benefits of facile synthesis and purification typical of small molecules with the low solubility characteristic of polymers, caused by their efficient packing in crystals.[16–18] Shape-persistent macrocycles have pre-engineered cavities in their structures and a severely limited conformational space.[19] Their solid-state structures are often porous, allowing the diffusion and transport of complex carrier ions.[20–22] In combination with electroactive groups in their structures, such porosity facilitates electrochemical kinetic processes in these materials.[23]

In this Communication, we report the synthesis and electrochemical investigations of tetrameric cyclotetrabenzil-based macrocycles **1**–**3** with eight carbonyl functional groups (Figure 1, see also Supporting Information), as well as compound **4**: the acyclic counterpart of **2** with only two carbonyl groups. The electrochemical results show that, despite structural similarity, compounds **1**–**3** behave very differently when included into organic battery electrodes. The naphthalene-based macrocycle **2** stands out as the only one to reversibly store up to eight electrons. The key to its superior performance is the shape-persistent structure, which ensures low solubility in the electrolyte throughout the redox cycling. This study offers important insights into

[*] J. Meng,[+] Dr. A. Robles,[+] Dr. S. Jalife,[+] Prof. Dr. J. I. Wu, Prof. Dr. O. Š. Miljanić
Department of Chemistry, University of Houston
3585 Cullen Blvd., Houston, TX-77204-5003 (USA)
E-mail: jiwu@central.uh.edu
miljanic@uh.edu

W. Ren[+]
Department of Chemical and Biomolecular Engineering, University of Houston
Houston, TX-77204-4004 (USA)

Y. Zhang, Dr. L. Zhao, Dr. Y. Liang, Prof. Dr. Y. Yao
Department of Electrical and Computer Engineering and Materials Science and Engineering Program, University of Houston
Houston, TX-77204 (USA)
and
Texas Center for Superconductivity at the University of Houston, University of Houston
Houston, TX-77204 (USA)
E-mail: yliang7@central.uh.edu
yyao4@central.uh.edu

[+] These authors contributed equally to this work.

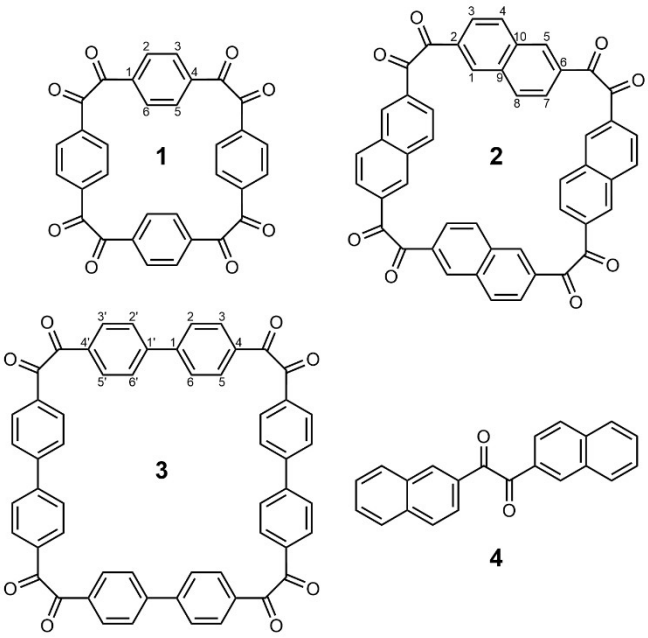


***Figure 1.*** Cyclotetrabenzil octaketone macrocycles **1**–**3** (with ring numbering schemes used in the text) and compound **4**, the acyclic monomeric counterpart of **2**.

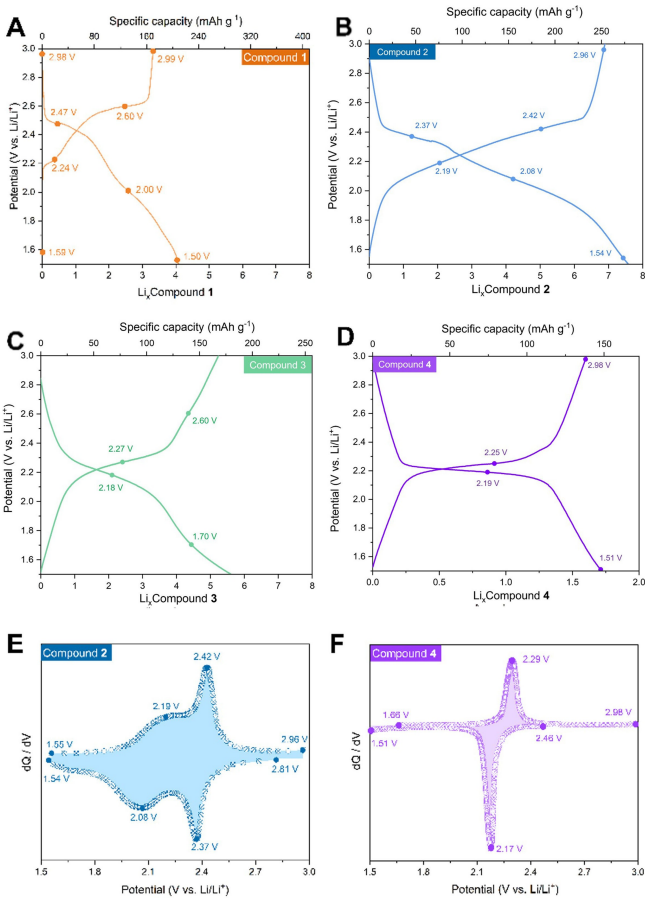


***Figure 2.*** Charging/discharging profiles of compounds **1** (A), **2** (B), **3** (C) and **4** (D). d*Q*/d*V* profiles of compounds **2** (E) and **4** (F) in the solution of LiTFSI in DME/DOL as the electrolyte.

the potential of shape-persistent, redox-active macrocyclic compounds[24] as privileged small-molecule motifs for the construction of organic electrode materials.

Macrocycle **1** has been previously reported,[25–27] while **2** and **3** have been prepared by the oxidation of expanded cyclotetrabenzoins.[28] The acyclic monomeric 1,2-bis(2-naphthyl)ethan-1,2-dione (**4**) was prepared by the oxidation of the corresponding benzoin, which was in turn produced by the benzoin condensation[29] of 2-formylnaphthalene. Compounds **1**–**4** are air-stable and contain either one or four pairs of redox-active carbonyl groups. Their spectroscopic characterization data are consistent with their symmetry; for all compounds, a single $^{13}C$ NMR signal for their carbonyl groups is observed, indicating their equivalence. From the crystal structures of analogs of **1**–**3**, central cavities with approximate dimensions of 6.8×6.8 Å (**1**), 8.6×8.6 Å (**2**), and 10.1×11.9 Å (**3**) are expected. Details of syntheses and spectroscopic properties of **2**–**4** are given in the Supporting Information.

With compounds **1**–**4** in hand, we evaluated their electrochemical redox behavior as the active components within the organic electrodes. Figure 2A–D show the charge/discharge profiles during typical cycling for compounds **1**–**4** under the current density of 100 mA g$^{-1}$, and using lithium bis-trifluoromethanesulfonimide (LiTFSI) in dioxolane/dimethoxyethane (DOL/DME) as the electrolyte. Assuming the transfer of eight electrons to their carbonyl groups, the theoretical specific capacities of compounds **1**–**3** are 406.02, 294.46, and 257.44 mAh g$^{-1}$, respectively. However, compound **1** showed a notably lower specific capacity of 171 mAh g$^{-1}$. Compound **3** displayed an irreversible discharging tail near the cut-off voltage. In contrast, the discharge capacity for **2** in a typical cycle was found to be 279 mAh g$^{-1}$ in a 3 M electrolyte solution (Figure 2B), which is ≈95 % of the theoretical capacity. This capacity confirmed that a molecule of **2** can reversibly store up to eight electrons during the electrochemical cycling; compounds **1** could store only up to four electrons. Similarly, compound **4** with two carbonyl groups exhibited the discharging capacity of 148.7 mAh g$^{-1}$ (Figure 2D), which also approached its predicted specific capacity of 172.7 mAh g$^{-1}$, confirming that all the carbonyl groups within the molecule are electrochemically active.

We ascribed the poorer performance of **3** to its higher solubility in the electrolyte, either in its neutral and/or partially reduced states. Macrocycle **3** has a large cavity space and thus free rotation of the biphenyl linkers can increase solubility, as suggested by a low computed rotational barrier (1.7 kcal mol$^{-1}$, cf. 12.0 kcal mol$^{-1}$ for **2** and 11.4 kcal mol$^{-1}$ for **1**). The reasons for the inferior performance of **1** are discussed below in the computational section. We therefore focused our further investigation on the best-performing macrocycle **2**, as well as its model compound **4**. The solubility of **2** in the 0.5 M solution of LiTFSI in DME/DOL electrolyte is 3.6±0.1 mmol L$^{-1}$, while that of **4** is 164±1 mmol L$^{-1}$ (Figure S11). The much lower solubility of

**2** is tentatively ascribed to its symmetric structure which facilitates crystal packing[18] and the free rotation of naphthalene moieties in the acyclic **4**.

For these two compounds, d$Q$/d$V$ vs. potential dependencies are plotted in Figures 2E, F, and S7 based on the charging/discharging profiles. Two pairs of redox peaks are observed for compound **2** (Figure 2E) at 2.37 and 2.08 V (for lithiation), suggesting that eight electrons are transferred in two separate steps; different shapes of these two pairs of peaks also indicate different electron transfer kinetics. In contrast, compound **4** only shows one pair of peaks in its d$Q$/d$V$ plot (2.17 V for lithiation, Figure 2F), indicating that it achieves all its capacity in an apparent one-step reaction.

To better understand the difference in the reaction mechanism between compounds **2** and **4**, we performed computational studies. DFT calculations for **2** and **4** and their reduced, $Li^+$-bound complexes were performed to provide insights into structural factors that influence the reduction behavior of the macrocycle versus its truncated acyclic model. Cyclotetrabenzoin macrocycle **2** undergoes a two-step eight-electron reduction process (Figure 3A). In the first step, four electrons add to **2** and four $Li^+$ ions bind to the four pairs of neighboring carbonyl groups, forming **2**-$Li_4$. In the second step, four more electrons are added to **2**-$Li_4$ and four more $Li^+$ ions bind to the four pairs of neighboring partially reduced carbonyl groups, forming a near-tetrahedral arrangement between the two Li and two O atoms in **2**-$Li_8$. In agreement with the experiment, vertical attachment of four electrons onto **2** is endothermic ($E_v$ = 6.2 eV, **2**→$\mathbf{2}^{4-}$), but the addition of the next four electrons to **2**-$Li_4$ is even more so ($E_v$ = 8.6 eV, **2**-$Li_4$→**2**-$Li^{4-}$; Figure 3C).

Computations show that reduction of **2** is localized at the four dicarbonyl sites. Notably, aromaticity of the naphthalene linkers remains intact throughout the reduction process (see computed nucleus independent chemical shifts, NICS, results in Figure S15). In **2**, all of the carbonyl-linking C–C bonds are formal single bonds (C–C = 1.538 Å, Wiberg bond index, WBI = 0.91, Figure 3C). Upon four-fold reduction to **2**-$Li_4$, four of the carbonyl groups (C=O) are converted to ketyl radical anions (•C–$O^-$), and the resulting allylic conjugation shortens the carbonyl-linking C–C bonds (C–C = 1.452 Å, WBI = 1.24). Complex **2**-$Li_4$ is a quintuplet ground state with spins localized on the carbonyl sites. In **2**-$Li_8$, the addition of the next four electrons reduces all of the carbonyl groups, forming eight C–$O^-$ anions, and the carbonyl-linking C–C bonds shorten even further, gaining pronounced π-bond character (C–C = 1.389 Å and WBI = 1.58). Eight electron reduction introduces a notable amount of strain into the macrocycle. In **2**-$Li_8$, the edge C–C bonds of each neighboring naphthalene linker are within the combined van der Waals radii of two C's (close contact [C···C] distances ranging from 3.071 to 3.373 Å, see geometries in the Figure S16), and increased rigidity of the carbonyl-linking C–C bonds precludes possible conformational changes that may relieve this repulsive interaction. The computed distortion energy ($\Delta E_{dist}$) for **2**-$Li_4$ is 14.0 kcal mol$^{-1}$, while that for **2**-$Li_8$ is 142.0 kcal mol$^{-1}$, showing significantly greater energetic penalty for reorienting the naphthalene linkers in **2**-$Li_8$ (Figure 3C). Values for $\Delta E_{dist}$ were estimated based on the single point total

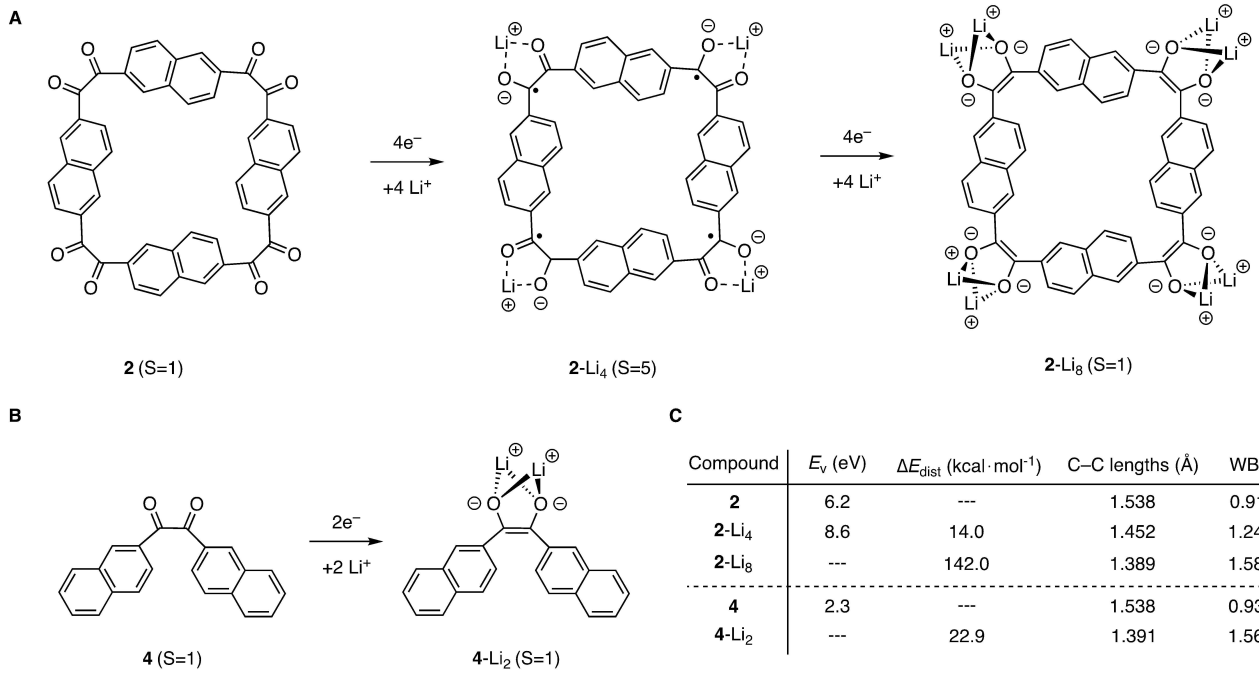


| Compound | $E_v$ (eV) | $\Delta E_{dist}$ (kcal·mol$^{-1}$) | C–C lengths (Å) | WBI |
|---|---|---|---|---|
| **2** | 6.2 | --- | 1.538 | 0.91 |
| **2**-$Li_4$ | 8.6 | 14.0 | 1.452 | 1.24 |
| **2**-$Li_8$ | --- | 142.0 | 1.389 | 1.58 |
| **4** | 2.3 | --- | 1.538 | 0.93 |
| **4**-$Li_2$ | --- | 22.9 | 1.391 | 1.56 |

***Figure 3.*** Proposed two-step 8$e^-$ reduction for **2** (A) and one-step 2$e^-$ reduction for **4** (B). Multiplicities ($S$) are show in parenthesis. C: Computed vertical 4$e^-$ and 2$e^-$ reduction energies ($E_v$) for the two-step reduction of **2**, **2**-$Li_4$, **2**-$Li_8$ and one-step reduction for **4**, **4**-$Li_2$. Computed distortion energies ($\Delta E_{dist}$), C–C bond lengths, and Wiberg bond indices (WBI) of the carbonyl-linking C–C bonds are also listed.

electronic energies of **2**-$Li_4$ and **2**-$Li_8$ with $Li^+$ ions removed minus the total electronic energies of $\mathbf{2}^{4-}$ and $\mathbf{2}^{8-}$, respectively. Computed noncovalent interaction (NCI) plots for **2**, **2**-$Li_4$, and **2**-$Li_8$ are given in the Supporting Information (Figure S17). Even though macrocycle **1** is structurally similar to **2**, the energetic penalty for $4e^-$ reduction is noticeably higher ($E_v = 8.7$ eV for **1**→$\mathbf{1}^{4-}$ and 12.0 eV for **1**-$Li_4$→**1**-$Li_4^{4-}$, cf. data in Figure 3C), possibly due to a smaller cavity space.

Acyclic compound **4** is a truncated fragment of **2** and undergoes a one-step two-electron reduction (Figure 3B). In **4**, the carbonyl groups form a 123.2° O–C–C–O dihedral angle. Upon twofold reduction, $Li^+$ ions bind to the two carbonyl groups forming a near-tetrahedral arrangement between the two Li and two O atoms. The reduced carbonyl groups are now in a cisoid conformation with a 6.2° O–C–C–O dihedral angle. Notably, vertical $2e^-$ attachment to **4** is less endothermic ($E_v = 2.3$ eV, **4**→$\mathbf{4}^{2-}$) than half of the vertical $4e^-$ attachment of **2** ($1/2\ E_v = 3.1$ eV, Figure 3C). The carbonyl-linking C–C bond is a formal single bond in **4** (C–C = 1.538 Å, WBI = 0.93) but shortens significantly in **4**-$Li_2$ (C–C = 1.391 Å, WBI = 1.56). In **4**-$Li_2$, the edge C–C bonds of each neighboring naphthalene linkers are within the combined van der Waals radii of two C's (close contact [C···C] distances ranging from 3.220 to 3.253 Å, see geometries in the Figure S16). However, the estimated distortion energy for **4**-$Li_2$ ($\Delta E_{dist} = 22.9$ kcal mol$^{-1}$) is less than a quarter of the distortion energy of **2**-$Li_8$ ($1/4\,\Delta E_{dist} = 35.5$ kcal mol$^{-1}$). These results explain the observed two-step reduction of macrocycle **2**. The addition of the first four electrons creates ketyl radical anions, which retain most of the conformational flexibility of the neutral **2**. Subsequent reductions are more difficult as they create strained and rigid dianions. We speculate that this progressive rigidification in the **2**→**2**-$Li_4$→**2**-$Li_8$ series also results in desirable lowered solubility of the reduced species relative to **2**.

Figure 4 demonstrates the galvanostatic cycling of compounds **2** and **4** in 3 M LiTFSI electrolyte at 1 C. Cathodes made with macrocycle **2** exhibit stable cycling with columbic efficiency ≈99 %. After 135 cycles, the discharge capacity retention of compound **2** is 65 %. It can be more clearly seen from Figure S7 that the capacity of compound **4** decays quickly due to its faster dissolution even in the 3 M electrolyte. In situ infrared spectra of **2** (Figure S14) show the C=O signal at wavenumbers between 1700 and 1600 cm$^{-1}$ disappearing during discharging and reappearing during charging, indicating good cycling reversibility of **2** as the organic cathode for lithium-ion storage.

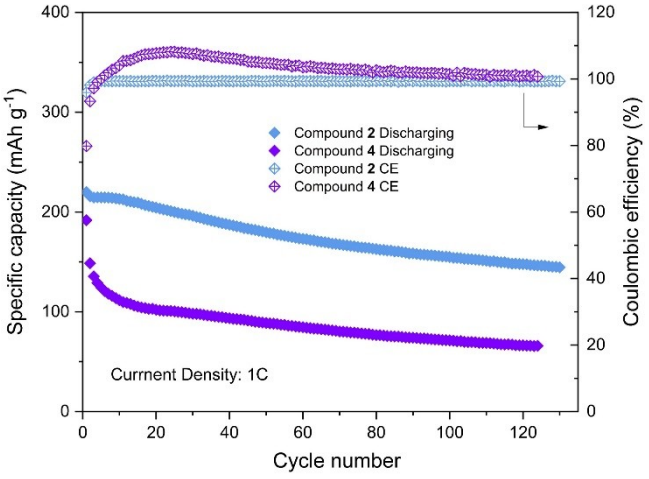


***Figure 4.*** Galvanostatic cycling of compounds **2** and **4** in a 3 M LiTFSI in DME/DOL electrolyte. 1 C equals 294.5 mA g$^{-1}$ for compound **2** and 172.7 mA g$^{-1}$ for compound **4**, respectively.

In conclusion, we have compared three cyclotetrabenzil octaketone macrocycles as organic cathode materials for lithium-ion storage. Among them, macrocycle **2** exhibits a desirable balance of electronic and rigid structural properties that support efficient electrode reactions. Compound **2** has a specific capacity of 279 mAh g$^{-1}$ from a reversible eight-electron reduction, and displays a good cycling performance with 65 % of the initial capacity retained after 135 cycles. Compared to other rigid carbonyl compounds,[15,30] the naphthalene-based cyclotetrabenzil octaketone **2** reported here demonstrated a low-capacity decay at a current density of 1 C, while maintaining a high-capacity higher than 150 mAh g$^{-1}$ over 120 cycles. Investigation of the fundamental electron transfer processes for **2** and **4** revealed that compound **2** undergoes an eight-electron reduction in two discrete steps, while **4** achieves full reduction in a single step. Computational studies suggest that macrocycle **2** experiences moderate macrocyclic strain in the first step of the reduction process, but significant strain in the second step. These results highlight the importance of modulating macrocyclic strain in the design of small molecule organic cathode materials. This study provides new insights into the role of ring strain, noncovalent interactions, and multi-electron transfer energies of organic electrode material design, and offers a kinetic understanding for well-designed macrocycles in electrochemical process.

## Acknowledgements

This work was supported by the University of Houston's National Centers Planning Award, the National Science Foundation (DMR-1904998 to O.Š.M., CHE-1751370 to J.I.W.), and the Sloan Research Foundation (FG-2020-12811 to J.I.W.). The authors acknowledge the use of the Carya/Opuntia/Sabine Cluster and the advanced support from the Research Computing Data Core at the University of Houston to carry out the research presented here.

## Conflict of Interest

The authors declare no conflict of interest.

## Data Availability Statement

The data that support the findings of this study are available in the Supporting Information of this article.

**Keywords:** Cyclotetrabenzil · Lithium-Ion Batteries · Macrocycles · Multielectron Transfer · Ring Strain

[1] S. Ha, K. T. Lee, *Nat. Energy* **2016**, *1*, 16057.
[2] M. Armand, J. M. Tarascon, *Nature* **2008**, *451*, 652–657.
[3] C. Wang, T. Liu, X. Yang, S. Ge, N. V. Stanley, E. S. Rountree, Y. Leng, B. D. McCarthy, *Nature* **2022**, *611*, 485–490.
[4] N. Choi, Z. Chen, S. A. Freunberger, X. Ji, Y. Sun, K. Amine, G. Yushin, L. F. Nazar, J. Cho, P. G. Bruce, *Angew. Chem. Int. Ed.* **2012**, *51*, 9994–10024.
[5] L. F. Nazar, M. Cuisinier, Q. Pang, *MRS Bull.* **2014**, *39*, 436–442.
[6] W. E. Gent, G. M. Busse, K. Z. House, *Nat. Energy* **2022**, *7*, 1132.
[7] Y. Li, Y. Lu, Y. Ni, S. Zheng, Z. Yan, K. Zhang, Q. Zhao, J. Chen, *J. Am. Chem. Soc.* **2022**, *144*, 8066–8072.
[8] Y. Liang, Z. Tao, J. Chen, *Adv. Energy Mater.* **2012**, *2*, 742–769.
[9] M. Walter, K. V. Kravchyk, C. Böfer, R. Widmer, M. V. Kovalenko, *Adv. Mater.* **2018**, *30*, 1705644.
[10] H. Gao, A. R. Neale, Q. Zhu, M. Bahri, X. Wang, H. Yang, Y. Xu, R. Clowes, N. D. Browning, M. A. Little, L. J. Hardwick, A. I. Cooper, *J. Am. Chem. Soc.* **2022**, *144*, 9434–9442.
[11] Z. Tie, Y. Zhang, J. Zhu, S. Bi, Z. Niu, *J. Am. Chem. Soc.* **2022**, *144*, 10301–10308.
[12] C. Zhang, *Nat. Energy* **2017**, *2*, 17149.
[13] Z. Tie, Z. Niu, *Angew. Chem. Int. Ed.* **2020**, *59*, 21293–21303.
[14] S. Zhang, S. Li, Y. Lu, *eScience* **2021**, *1*, 163–177.
[15] D. Chen, A. Avestro, Z. Chen, J. Sun, S. Wang, M. Xiao, Z. Erno, M. M. Algaradah, M. S. Nassar, K. Amine, Y. Meng, J. F. Stoddart, *Adv. Mater.* **2015**, *27*, 2907–2912.
[16] S. D. Appavoo, S. Huh, D. B. Diaz, A. K. Yudin, *Chem. Rev.* **2019**, *119*, 9724–9752.
[17] Q. He, G. I. Vargas-Zúñiga, S. H. Kim, S. K. Kim, J. L. Sessler, *Chem. Rev.* **2019**, *119*, 9753–9835.
[18] M. I. Hashim, H. T. M. Le, T.-H. Chen, Y.-S. Chen, O. Daugulis, C.-W. Hsu, A. J. Jacobson, W. Kaveevivitchai, X. Liang, T. Makarenko, O. Š. Miljanić, I. Popovs, H. V. Tran, X. Wang, C.-H. Wu, J. I. Wu, *J. Am. Chem. Soc.* **2018**, *140*, 6014–6026.
[19] M. Al Kobaisi, S. V. Bhosale, K. Latham, A. M. Raynor, S. V. Bhosale, *Chem. Rev.* **2016**, *116*, 11685–11796.
[20] S. Eder, D. J. Yoo, W. Nogala, M. Pletzer, A. Santana Bonilla, A. J. P. White, K. E. Jelfs, M. Heeney, J. W. Choi, F. Glöcklhofer, *Angew. Chem. Int. Ed.* **2020**, *59*, 12958–12964.
[21] D. J. Yoo, M. Heeney, F. Glöcklhofer, J. W. Choi, *Nat. Commun.* **2021**, *12*, 2386.
[22] K. W. Nam, H. Kim, Y. Beldjoudi, T. W. Kwon, D. J. Kim, J. F. Stoddart, *J. Am. Chem. Soc.* **2020**, *142*, 2541–2548.
[23] D. J. Kim, K. R. Hermann, A. Prokofjevs, M. T. Otley, C. Pezzato, M. Owczarek, J. F. Stoddart, *J. Am. Chem. Soc.* **2017**, *139*, 6635–6643.
[24] W. Zhang, J. S. Moore, *Angew. Chem. Int. Ed.* **2006**, *45*, 4416–4439.
[25] M. Alrayyani, O. Š. Miljanić, *Chem. Commun.* **2018**, *54*, 11989–11997.
[26] Q. Ji, H. T. M. Le, X. Wang, Y. S. Chen, T. Makarenko, A. J. Jacobson, O. Š. Miljanić, *Chem. Eur. J.* **2015**, *21*, 17205–17209.
[27] S. Hahn, M. Alrayyani, A. Sontheim, X. Wang, F. Rominger, O. Š. Miljanić, U. H. F. Bunz, *Chem. Eur. J.* **2017**, *23*, 10543–10550.
[28] A. M. Eisterhold, T. Puangsamlee, S. Otterbach, S. Bräse, P. Weis, X. Wang, K. V. Kutonova, O. Š. Miljanić, *Org. Lett.* **2021**, *23*, 781–785.
[29] L. E. Harrington, J. F. Britten, D. W. Hughes, A. D. Bain, J.-Y. Thépot, M. J. McGlinchey, *J. Organomet. Chem.* **2002**, *656*, 243–257.
[30] Z. Luo, L. Liu, Q. Zhao, F. Li, J. Chen, *Angew. Chem. Int. Ed.* **2017**, *56*, 12561–12565.

Manuscript received: January 17, 2023
Accepted manuscript online: April 17, 2023
Version of record online: ■■, ■■

# Communications

## Li-Ion Batteries

J. Meng, A. Robles, S. Jalife, W. Ren, Y. Zhang, L. Zhao, Y. Liang,* J. I. Wu,* O. Š. Miljanić,* Y. Yao* e202300892

Cyclotetrabenzil Derivatives for Electrochemical Lithium-Ion Storage

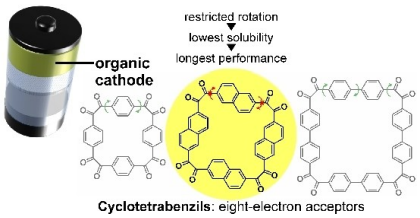


Naphthalene-based cyclotetrabenzil octaketone is an excellent cathode material for lithium-ion batteries. It reversibly accepts eight electrons per molecule, has a specific capacity of 279 mAh $g^{-1}$, and shows stable cycling performance with ≈65% retention after 135 cycles. Its shape-persistent, symmetric structure rigidifies during an eight-electron reduction, ensuring that this macrocycle remains insoluble in various redox states.